MOLECULAR ONCOLOGY 10 (2016) 344–359

available at www.sciencedirect.com

ScienceDirect

www.elsevier.com/locate/molonc

Transcription factor activating protein 2 beta (TFAP2B) mediates noradrenergic neuronal differentiation in neuroblastoma

Fakhera Ikram[a,b,c], *Sandra Ackermann*[a,b], *Yvonne Kahlert*[a,b], *Ruth Volland*[a,b], *Frederik Roels*[a,b], *Anne Engesser*[a,b], *Falk Hertwig*[a,b], *Hayriye Kocak*[a,b], *Barbara Hero*[a,b], *Daniel Dreidax*[d], *Kai-Oliver Henrich*[d], *Frank Berthold*[a,b], *Peter Nürnberg*[b,c], *Frank Westermann*[d], *Matthias Fischer*[a,b,e,*]

[a]*Department of Pediatric Oncology and Hematology, University Children's Hospital of Cologne, Germany*
[b]*Center for Molecular Medicine Cologne (CMMC), University of Cologne, Germany*
[c]*Cologne Center for Genomics (CCG), University of Cologne, Germany*
[d]*Division Neuroblastoma Genomics (B087), German Cancer Research Center, Heidelberg, Germany*
[e]*Max Planck Institute for Metabolism Research, Cologne, Germany*

ARTICLE INFO

Article history:
Received 23 April 2015
Received in revised form
5 October 2015
Accepted 23 October 2015
Available online 7 November 2015

Keywords:
TFAP2B
Neuroblastoma
Differentiation
Prognostic marker
Retinoic acid

ABSTRACT

Neuroblastoma is an embryonal pediatric tumor that originates from the developing sympathetic nervous system and shows a broad range of clinical behavior, ranging from fatal progression to differentiation into benign ganglioneuroma. In experimental neuroblastoma systems, retinoic acid (RA) effectively induces neuronal differentiation, and RA treatment has been therefore integrated in current therapies. However, the molecular mechanisms underlying differentiation are still poorly understood. We here investigated the role of transcription factor activating protein 2 beta (TFAP2B), a key factor in sympathetic nervous system development, in neuroblastoma pathogenesis and differentiation. Microarray analyses of primary neuroblastomas (n = 649) demonstrated that low *TFAP2B* expression was significantly associated with unfavorable prognostic markers as well as adverse patient outcome. We also found that low *TFAP2B* expression was strongly associated with CpG methylation of the *TFAP2B* locus in primary neuroblastomas (n = 105) and demethylation with 5-aza-2′-deoxycytidine resulted in induction of *TFAP2B* expression *in vitro*, suggesting that *TFAP2B* is silenced by genomic methylation. Tetracycline inducible re-expression of TFAP2B in IMR-32 and SH-EP neuroblastoma cells significantly impaired proliferation and cell cycle progression. In IMR-32 cells, TFAP2B induced neuronal differentiation, which was accompanied by up-regulation of the catecholamine biosynthesizing enzyme genes *DBH* and *TH*, and down-regulation of *MYCN* and *REST*, a master repressor of neuronal genes. By contrast, knockdown of *TFAP2B* by lentiviral transduction of shRNAs abrogated

Abbreviations: TFAP2B, transcription factor activating protein 2 beta; DAC, 5-aza-2′-deoxyctidine; RA, retinoic acid; INSS, International Neuroblastoma Staging System; INPC, International Neuroblastoma Pathology Committee; *MAP2*, microtubule associated protein 2; *NEFM*, neurofilament middle chain; NSE, neuron specific enolase; SYP, synaptophysin; TUBB3, class III beta-tubulin; EFS, event-free survival; OS, overall survival.

* *Corresponding author*. University Children's Hospital of Cologne, Department of Pediatric Oncology, Kerpener Str. 62, 50924 Cologne, Germany. Tel.: +49 221 478 6816; fax: +49 221 478 4689.
E-mail address: matthias.fischer@uk-koeln.de (M. Fischer).

http://dx.doi.org/10.1016/j.molonc.2015.10.020

RA-induced neuronal differentiation of SH-SY5Y and SK-N-BE(2)c neuroblastoma cells almost completely. Taken together, our results suggest that TFAP2B is playing a vital role in retaining RA responsiveness and mediating noradrenergic neuronal differentiation in neuroblastoma.

1. Introduction

Neuroblastoma is a pediatric cancer deriving from embryonal precursor cells of the sympathetic nervous system. The clinical and biological behavior of this tumor is remarkably heterogeneous, ranging from fatal tumor progression to spontaneous regression or differentiation into mature ganglioneuroma. A more differentiated histological phenotype of the tumor cells is associated with favorable patient outcome (Cohn et al., 2009). Likewise, low and high risk neuroblastomas exhibit distinct expression patterns of neuronal genes (Fischer et al., 2006; Fredlund et al., 2008; Ohira et al., 2005). Retinoic acid (RA) has been shown to effectively induce differentiation of neuroblastoma cells in experimental systems (Sidell, 1982), and is currently being used in maintenance treatment strategies for high risk neuroblastoma patients to prevent relapse (Matthay et al., 2009). However, the benefit of RA treatment in the clinical setting appears to be limited (Reynolds et al., 2003), and biomarkers that may predict response to RA therapy are lacking to date (Matthay et al., 2009).

Transcription factor activating proteins (TFAP2) are belonging to a sequence-specific DNA binding transcription factor family, which are encoded by five different but closely related genes, *TFAP2-A, B, C, D* and *E*. TFAP2 family members form homo- and heterodimers, and transactivate target genes by binding to GC-rich consensus elements (Eckert et al., 2005). TFAP2 proteins are RA-inducible transcriptional activators (Luscher et al., 1989), and have been shown to play important roles during vertebrate development, cell growth and differentiation (Auman et al., 2002; Moser et al., 1997; Zeng et al., 1997; Zhang et al., 1996). In addition, alterations in *TFAP2* expression patterns and both oncogenic and tumor suppressive functions have been described in various cancer entities (Fu et al., 2014; Pellikainen and Kosma, 2007). In neuroblastoma, expression of the *TFAP2* gene family member *TFAP2B*, also known as AP-2β, has been shown to be associated with low risk disease in small tumor cohorts (Fischer et al., 2006; Thorell et al., 2009). In vertebrate embryogenesis, *TFAP2B* is expressed in migrating neural crest cells and fetal sympathetic neuroblasts, and has been implicated in the development of the sympathetic nervous system (De Preter et al., 2006; Hong et al., 2011, 2008; Schmidt et al., 2011). These findings prompted us to investigate the role of TFAP2B in neuroblastoma pathogenesis and differentiation.

Here, we examined the expression of *TFAP2B* in a cohort of 649 primary neuroblastomas using microarrays, and assessed its correlation with prognostic markers and patient outcome. To investigate the mechanisms behind *TFAP2B* deregulated expression, we determined copy number alterations and DNA methylation patterns of the *TFAP2B* locus by array-CGH and methylation array analysis, respectively. The functional relevance of TFAP2B expression was determined by retroviral *TFAP2B* re-expression and shRNA-mediated *TFAP2B* knockdown in neuroblastoma cell lines. We found that low *TFAP2B* expression is associated with poor outcome and DNA methylation of the *TFAP2B* locus in primary neuroblastoma, and that TFAP2B mediates noradrenergic neuronal differentiation of neuroblastoma cells *in vitro*.

2. Materials and methods

2.1. Patient characteristics

A total of 649 primary neuroblastomas from 9 different countries (Germany, n = 492; USA, n = 59; Italy, n = 23; Japan, n = 20; France, n = 19; Spain, n = 14; Israel, n = 12; Belgium, n = 5; UK, n = 5) were analyzed by expression microarrays as described (Kocak et al., 2013). Stages were classified according to the International Neuroblastoma Staging System (INSS) (Brodeur et al., 1993): stage 1, n = 153; stage 2, n = 113; stage 3, n = 91; stage 4, n = 214; and stage 4S, n = 78. Patient's age at diagnosis ranged from 0 to 25.4 years (median age, 1.1 years). *MYCN* amplification was observed in 93 tumors, while it was absent in 550 tumors (not determined, n = 6). Loss of chromosome 1p was observed in 141 tumors, while normal chromosome 1p status was found in 411 tumors (not determined, n = 97). Risk estimation of the patients was performed according to NB2004 (low risk, n = 353; intermediate risk, n = 61; high risk, n = 210; unclassified, n = 25). Histological assessment was available for 376 neuroblastomas according to the International Neuroblastoma Pathology Committee (INPC) (Shimada et al., 1999): undifferentiated, n = 22; poorly differentiated, n = 311; and differentiating, n = 43. Prognostic gene expression-based classification of primary neuroblastomas was performed according to the recently developed prognostic classifier SVM_th10 (favorable, n = 363; unfavorable n = 211; unclassified, n = 75) (Oberthuer et al., 2015).

The neuroblastoma cohort analyzed by aCGH consisted of 199 primary tumors derived from German patients (stage 1, n = 40; stage 2, n = 33; stage 3, n = 38; stage 4, n = 60; and stage 4S, n = 28) (Kocak et al., 2013). Patient's age at diagnosis ranged from 0 to 25.4 years (median age, 1 year). *MYCN* amplification was observed in 23 tumors, while it was absent in 174 tumors (not determined, n = 2). According to NB2004, 107 patients of the cohort were classified as low risk, 31 as intermediate risk, and 59 as high risk.

The neuroblastoma cohort analyzed by methylation arrays consisted of 105 tumors derived from German patients (stage 1, n = 10; stage 2, n = 9; stage 3, n = 10; stage 4, n = 56; and stage 4S, n = 20). Patient's age at diagnosis ranged from 0 to 24.6 years (median age, 1 year). *MYCN* amplification was observed in 33 tumors, while it was absent in 72 tumors. According to NB2004, 40 patients of the cohort were classified as low risk, 9 as intermediate risk, and 56 as high risk.

2.2. Analysis of TFAP2B expression patterns and genetic and epigenetic alterations of the TFAP2B locus

Single-color gene expression profiles from neuroblastoma samples and cell lines were generated using 44K oligonucleotide microarrays as described previously (Kocak et al., 2013; Oberthuer et al., 2010). Array-based comparative genomic hybridization (aCGH) using 44K or 105K microarrays was used to determine DNA copy number profiles from 199 neuroblastoma tumors as described (Fischer et al., 2010; Kocak et al., 2013; Spitz et al., 2006). All gene expression and aCGH data are available at Gene Expression Omnibus (Accessions: GSE45480, GSE74350 and GSE25771). Whole-genome DNA methylation profiles of 105 neuroblastoma tumors were generated using the Infinium HumanMethylation450 BeadChip (Illumina) according to the manufacturers' instructions.

2.3. Cell culture

The neuroblastoma cell lines SH-SY5Y, SK-N-DZ, SK-N-AS, CHP-212 and SH-EP were obtained from American Tissue Culture Collection (ATCC, Rockville, MD, USA), and the neuroblastoma cell lines IMR-32, LAN-5, NMB, GI-ME-N and NBL-S were purchased from DSMZ-German Collection of Microorganisms and Cell Cultures (Braunschweig, Germany). KELLY and SK-N-BE(2)c cells were provided by Dr. Olaf Witt, German Cancer Research Center (DKFZ), Heidelberg (Germany), and CLB-GA by Dr. Johannes Schulte, University Children's Hospital, Essen (Germany), and were validated by the DSMZ using STR profiling. Neuroblastoma cells were maintained in media according to the instructions from suppliers supplemented with 10–20% fetal calf serum (FCS) (Invitrogen, Germany). Inducible cell lines were maintained in RPMI-1640 supplemented with 10% Tet-free FCS (PAA, Germany), 50 μg/ml G418 and 30–50 μg/ml Hygromycin B. PT67 packaging cells were obtained from Clontech Laboratories and grown in DMEM supplemented with 10% FCS. Cells were maintained in a humidified incubator at 37 °C with 5% CO_2 and passaged at 90% confluence using Trypsin-EDTA. Doxycycline (Sigma–Aldrich, Taufkirchen, Germany) was used at 2 μg/ml and 1 μg/ml to induce transgene expression in SH-EP cells and IMR-32 cells, respectively. Neuroblastoma cell lines were shown to be free of mycoplasma by using the Venor® GeM Mycoplasma Detection Kit (Minerva Biolabs, Berlin, Germany) according to the manufacturer's protocol. To assess RA-mediated differentiation, all-trans retinoic acid (Sigma–Aldrich) was dissolved in ethanol, and used at 1 μmol/L for 6–18 days in diffused light. Ethanol treated cells were used as negative control. To assess the effects of demethylation, IMR-32 cells were grown in the presence of 3 μM 5-aza-2′-deoxycytidine (DAC; Sigma–Aldrich) or DMSO (control) for 3–7 days. Media was changed every 24 h containing fresh DAC.

2.4. Cloning of TFAP2B into the pRevTRE vector and generation of TFAP2B inducible neuroblastoma cell lines

A human *TFAP2B* full open reading frame was obtained by PCR from the pCMV-Sport6ccdB vector (RZPD) and cloned into the pRevTRE vector (Clontech, Heidelberg, Germany). Neuroblastoma cell lines stably expressing either *TFAP2B* or *GFP* under the control of the reverse tetracycline-controlled transactivator were generated using the RevTet System (Clontech) as described elsewhere (Kocak et al., 2013). Three single clones for SH-EP pRevTet-On/pRevTRE-*TFAP2B* cells were generated, and all experiments were performed with these clones. Promoter leakage of *TFAP2B* expression was observed in IMR-32 pRevTet-On/pRevTRE-*TFAP2B* cells without doxycycline. Therefore, IMR-32 pRevTet-On/pRevTRE-*GFP* cells were used as control.

2.5. Lentivirus production and infection of neuroblastoma cells

Four short hairpin RNAs targeting the *TFAP2B* gene were obtained from Sigma–Aldrich (Supplementary Table S1). Replication-incompetent lentiviruses were produced using the *pLKO.1* vector by co-transfection with *Δ8.91* and *pHIT-VSV-G* in HEK 293T cells using TRANS-IT (Mirus). Infectious lentiviruses were harvested 48 h post-transfection, centrifuged to remove cell debris, and then filtered through 0.45 μm cellulose acetate filters. Recombinant lentiviruses plus 10 μg/ml of polybrene were used to infect exponentially growing neuroblastoma cells. After transduction, SK-N-BE(2)c and SH-SY5Y cells were selected with 2 μg/ml puromycin and 1 μg/ml puromycin, respectively.

2.6. Western blot hybridization and RT–qPCR

Immunoblots were prepared as described previously (Nowacki et al., 2008). Total protein extracts were isolated either with RIPA or Cell Lysis Buffer (Cell Signaling Technology). RT-qPCR was carried out two times in technical triplicates as described previously (Fischer et al., 2005). Results of one independent experiment are shown. Primer sequences are given in Supplementary Table S2.

2.7. Analysis of cell cycle distribution, cell growth and senescence

Cell proliferation was assessed using the trypan blue exclusion test. Cells were harvested at days 2, 4, 6 and 8, and evaluated for the number and viability by trypan blue exclusion using a Cedex cell counter (Roche). Cell cycle distribution was assessed by flow cytometry (FACS Canto; BD Biosciences) and analyzed using the DIVA software (BD Biosciences). To examine senescence, cells were fixed and stained using the SA-ß-Gal kit (Cell Signaling Technology) according to the manufacturer's instructions.

2.8. Immunohistochemistry, immunofluorescence and microscopy

To assess the tumor cell content in primary neuroblastomas, we performed immunohistochemistry staining using the NB84 monoclonal antibody, which has been established as a useful tool for differential diagnosis of neuroblastoma (Miettinen et al., 1998; Thomas et al., 1991). Sections were fixed in acetone for 5 min and stained with NB84 (Leica Biosystems) using the EnVision™ G|2 System/AP (DAKO); consecutive sections were then stained with rabbit-anti-TFAP2B for immunofluorescence (Cell Signaling Technology). For immunofluorescence of cell lines, cells were grown in chamber slides (Nunc Lab-Tek II Chamber Slide* System, Thermo Scientific), fixed with 4% paraformaldehyde and stained with primary antibody rabbit-anti-TFAP2B (1:100; Cell Signaling Technology), rabbit-anti-MAP2 (1:200; Santa Cruz) or mouse-anti-TUBB3 (1:200, Santa Cruz). TFAP2B and MAP2 signals were detected either by anti-rabbit IgG (H+L), $F(ab')_2$ Fragment Alexa Fluor® 488 Conjugate, or by anti-rabbit IgG (H+L), $F(ab')_2$ Fragment Alexa Fluor® 555 Conjugate (Cell Signaling Technology). TUBB3 signals were detected by anti-mouse-IgG conjugated with TRITC (DAKO). Nuclei were stained with 4′,6-diamidino-2-phenylindole (DAPI), and actin filaments were labeled with rhodamine phalloidin. Fluorescent images were taken with a confocal microscope and FV 1000 software (Olympus Fluoview FV 1000) or widefield microscope Leica DMI6000 B.

2.9. Data analysis and statistics

Analysis of associations between *TFAP2B* expression levels and prognostic markers or outcome was performed using SPSS version 20.0 (IBM, Mainz, Germany) and R version 2.15.0. Two-tailed non-parametric tests (Mann–Whitney U-test and Kruskal-Wallis test) were used where appropriate. To assess the prognostic value of *TFAP2B* expression levels, the neuroblastoma cohort was randomly divided into training and test sets. The optimal cut-off expression level was calculated by means of maximally selected rank statistics in the training cohort. The optimal cut-off was defined as the intensity value of *TFAP2B* that separates the cohort best in two groups in terms of overall-survival (OS) (Hothorn and Lausen, 2002). The prognostic value of the *TFAP2B* cut-off value was then assessed in the validation cohort by Kaplan-Meier survival analysis using log-rank test (both for event-free survival (EFS) and OS), and multivariate Cox regression analysis. The factors age (>18 months *versus* <18 months), tumor stage (stage 4 *versus* stages 1–3 and 4S), *MYCN* (amplified *versus* normal) and *TFAP2B* expression were fitted into a stepwise-backward selection model. The likelihood ratio test p for inclusion was $\leq$0.05 and for exclusion was $\geq$0.1. Recurrence, progression and death from disease were considered as events.

To describe the association between CpG methylation and gene expression, methylation cut-off values for dichotomization of *TFAP2B* expression and p-values were estimated by maximally selected log-rank statistics (Lausen and Schumacher, 1992). The Wilcoxon rank-sum test was used to test for an association between *TFAP2B* methylation and established prognostic factors.

Gene Set Enrichment Analysis (GSEA) (www.broadinstitute.org/gsea/; Subramanian et al., 2005) was used to generate enrichment plot of the gene set in the Biocarta cell cycle pathway in *TFAP2B* and *GFP* expressing IMR-32 cells.

Quantitative data of functional analyses are given as means ±S.D. Unpaired two-tailed student's t-tests were used where appropriate. The difference was considered to be significant at $p < 0.05$.

3. Results

3.1. Low TFAP2B expression is associated with unfavorable prognostic markers and poor outcome in neuroblastoma

To investigate whether *TFAP2B* is associated with prognostic variables in neuroblastoma, we determined *TFAP2B* expression levels by microarrays in a cohort of 649 primary neuroblastomas representing the entire spectrum of the disease. We observed that low *TFAP2B* expression was associated with prognostic markers of poor outcome including age of the patient at diagnosis >18 months, stage 4 disease, *MYCN* amplification, loss of chromosome 1p and high risk disease according to the criteria of the German NB2004 trial ($p < 0.001$ each, Figure 1a–e). Low *TFAP2B* expression was also associated with unfavorable gene expression-based outcome prediction using an accurate multigene expression classifier that we have developed recently ($p < 0.001$, Figure 1f) (Oberthuer et al., 2015). To assess the impact of *TFAP2B* expression on neuroblastoma patient outcome, we divided the entire cohort randomly into halves, and determined the optimal prognostic expression threshold in the first set (Supplementary Figure S1). The prognostic value of *TFAP2B* was then evaluated in the second set. We found that low *TFAP2B* expression was strongly associated with adverse patient outcome for both event-free survival (EFS at 5 years, 0.79 ± 0.03 *vs* 0.45 ± 0.04, $p < 0.001$; Figure 1g) and overall-survival (OS at 5 years, 0.91 ± 0.02 *vs* 0.63 ± 0.04, $p < 0.001$; Figure 1h). In addition, multivariate Cox regression models based on EFS and OS considering established risk markers (*MYCN* status, tumor stage and patient age at diagnosis) identified *TFAP2B* expression as a significant independent prognostic variable for EFS (Table 1). Together, our results demonstrate that high *TFAP2B* transcript levels are associated with a favorable neuroblastoma phenotype, pointing towards its potential biological relevance.

To determine whether TFAP2B expression is also associated with outcome in RA-treated patients, we selected all German high-risk patients who had received megatherapy with autologous stem cell transplantation and had been event-free for at least 3 months after megatherapy ($n = 89$). In the RA treated subgroup ($n = 73$), we observed that patients whose tumors had higher *TFAP2B* expression levels had a significantly better EFS than those with lower *TFAP2B* expression (5-year EFS 0.77 ± 0.12 *vs* 0.36 ± 0.06, $p = 0.025$; Supplementary Figure S2). Similarly, there was a trend

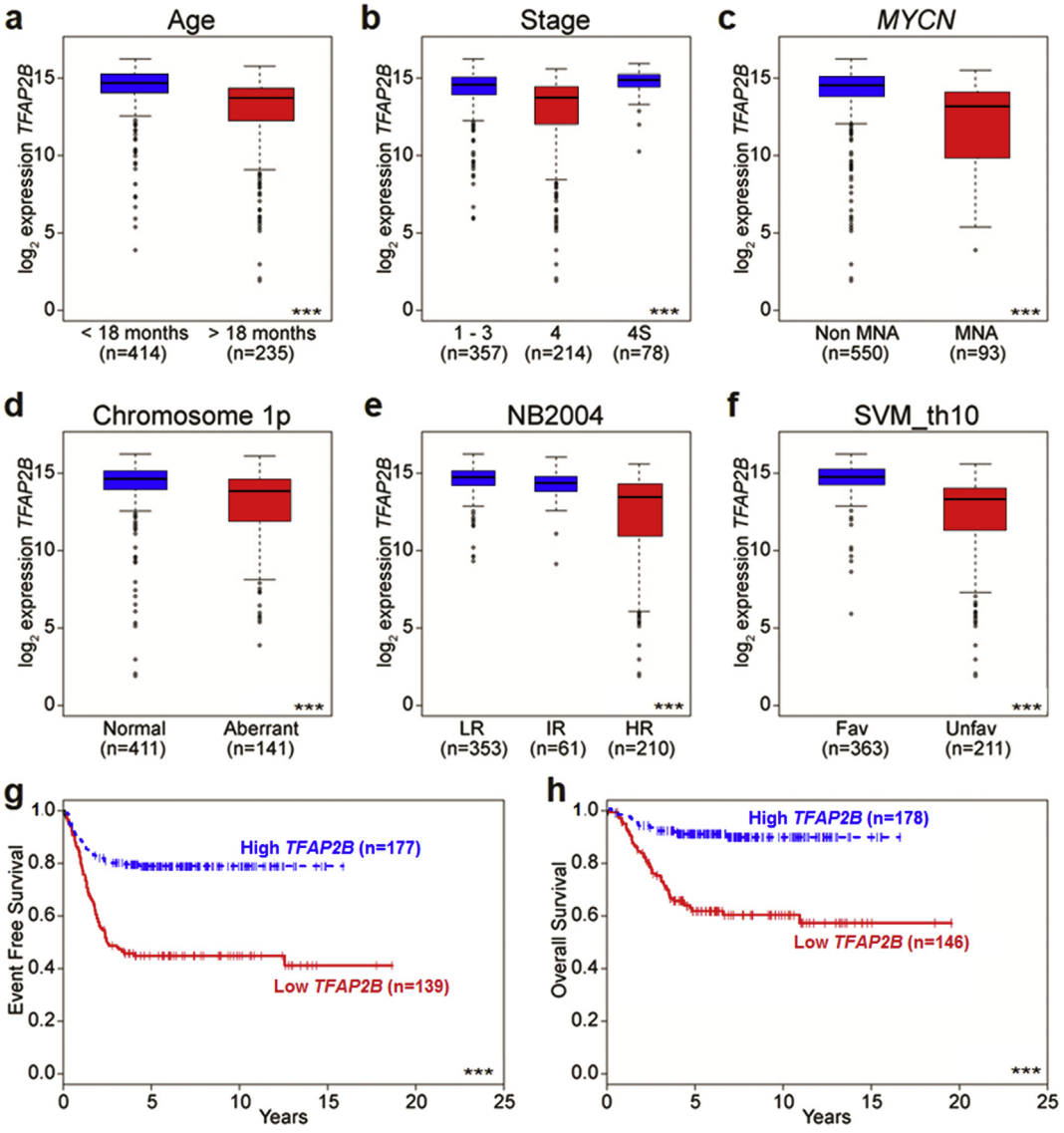

Figure 1 – Association of *TFAP2B* expression levels with prognostic markers and outcome in neuroblastoma. Association of (a) age at diagnosis, (b) tumor stage, (c) *MYCN* amplification status, (d) chromosome 1p status, (e) risk stratification according to NB2004, and (f) gene expression-based classification (according to the SVM_th10 classifier) with *TFAP2B* transcript levels in 649 neuroblastoma samples as determined by microarray gene expression analysis. Boxes, median expression values (horizontal line) and 25th and 75th percentiles; whiskers, distances from the end of the box to the largest and smallest observed values that are < 1.5 box lengths from either end of the box; circles, outliers. (g) EFS and (h) OS of neuroblastoma patients in the validation set according to the prognostic *TFAP2B* expression cut-off determined in the training set. n = patient number; (***), $p < 0.001$.

towards a better OS in this cohort (5-year OS 0.85 ± 0.10 *vs* 0.56 ± 0.07, p = 0.091). By contrast, *TFAP2B* expression did not distinguish patients with different outcome in the small subgroup without RA treatment (n = 16; 5-year EFS, 0.50 ± 0.20 *vs* 0.43 ± 0.19, p = 0.554; 5-year OS, 0.50 ± 0.20 *vs* 0.43 ± 0.19, p = 0.536). While these results have to be validated in larger cohorts, they may indicate that *TFAP2B* expression might serve as a biomarker to predict RA treatment success.

We also assessed whether *TFAP2B* expression is associated with the degree of morphological differentiation in primary neuroblastomas. We observed that poorly differentiated tumors had higher *TFAP2B* expression levels than both undifferentiated and differentiating tumors (Supplementary Figure S3a). On the molecular level, we noticed that *TFAP2B* expression was significantly correlated with gene expression of the catecholamine biosynthesizing enzymes dopamine beta hydroxylase (*DBH*) and tyrosine hydroxylase (*TH*), indicating that TFAP2B might up-regulate expression of these enzymes in neuroblastoma (Supplementary Figure S3b and S3c).

3.2. *Analysis of genetic and epigenetic alterations of the* TFAP2B *locus*

We next aimed at investigating whether genetic or epigenetic alterations of the *TFAP2B* locus are associated with aberrant *TFAP2B* expression. First, we examined the *TFAP2B*

Table 1 – Multivariate Cox regression models based on EFS and OS considering single prognostic markers and *TFAP2B* expression.

Marker	Patient (N)	Available cases (N)	Hazard ratio	95% CI	P-value
Model based on EFS	324	312			
Age (≥18 months *versus*< 18 months)			2.97	1.84; 4.79	<0.001
Stage (4 *versus* 1–3, 4S)			1.64	1.06; 2.55	0.026
MYCN (amplified *versus* normal)			1.65	1.05; 2.59	0.035
TFAP2B (<19830.07 *versus* ≥19830.07)			1.59	1.01; 2.52	0.042
Model based on OS	324	320			
Age (≥18 months *versus* < 18 months)			5.92	2.90; 12.07	<0.001
Stage (4 *versus* 1–3, 4S)			2.53	1.38; 4.63	0.002
MYCN (amplified *versus* normal)			3.72	2.23; 6.20	<0.001
TFAP2B (<19830.07 *versus* ≥19830.07)					n.s.

HR, Hazard ratio; n.s., not significant.

methylation status using global methylation profiles of 105 primary neuroblastomas, which were generated by microarrays containing probes for 450K CpG sites. We observed a significant correlation between *TFAP2B* CpG methylation and low transcript expression levels (Supplementary Table S3), with strongest correlations seen for two CpG sites close to the transcription start site and one CpG site in exon 2 ($p < 0.001$ each; Figure 2a and 2b). Increased methylation levels of these CpG sites were found to be significantly associated with prognostic variables of poor outcome including *MYCN* amplification, stage 4, age of the patient at diagnosis >18 months and allocation to the high risk group according to the German

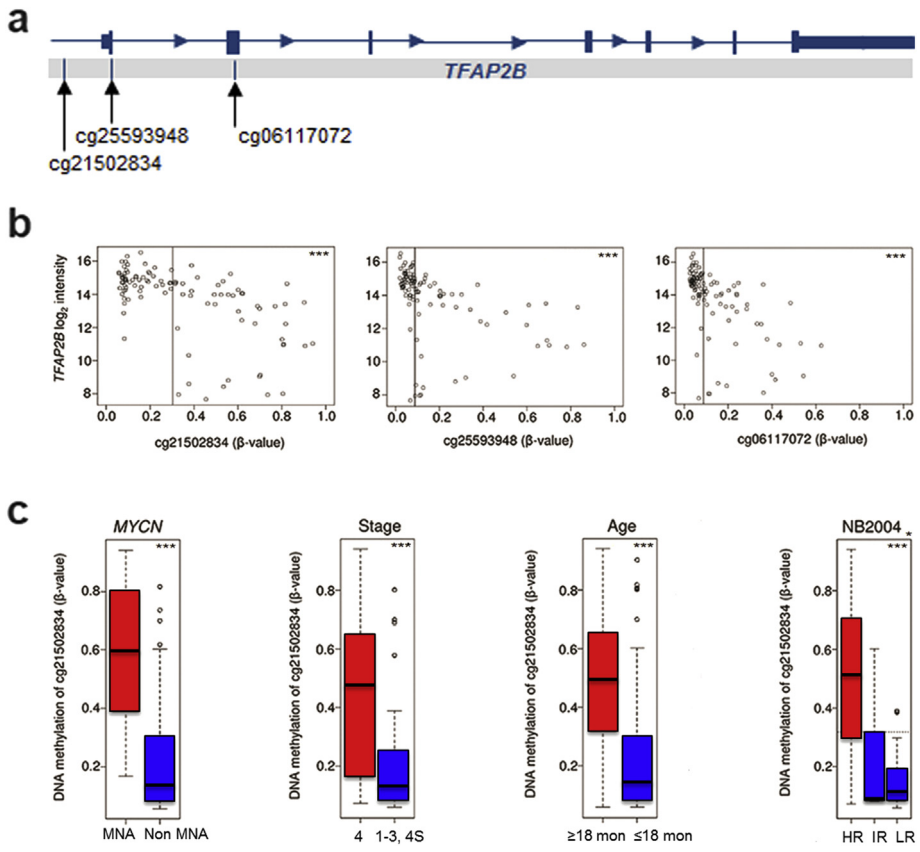

Figure 2 – Association of CpG methylation of the *TFAP2B* locus with prognostic markers and *TFAP2B* expression in neuroblastoma. (a) *TFAP2B* genomic structure and localization of CpGs analyzed. (b) Correlation of *TFAP2B* methylation with *TFAP2B* expression. Log intensities of probe A_24_P20954 (*TFAP2B* expression) are plotted against β-values of probes cg21502834, cg06117072 and cg25593948 representing CpGs in the 5′ region of the *TFAP2B* locus. (c) Association of *TFAP2B* methylation (probe cg21502834) with *MYCN* amplification status, tumor stage, age at diagnosis, and risk group according to NB2004 in 105 neuroblastoma samples as determined by 450K methylation arrays. Boxes, median expression values (horizontal line) and 25th and 75th percentiles; whiskers, distances from the end of the box to the largest and smallest observed values that are < 1.5 box lengths from either end of the box; circles, outliers. (*), Wilcoxen test (HR vs IR/LR); (***), $p < 0.001$; MNA, *MYCN*-amplified tumors.

NB2004 risk estimation system ($p < 0.001$ each; Figure 2c and Supplementary Figure S4. Together, these results suggest that low expression of *TFAP2B* in high risk neuroblastoma might be due to CpG methylation of the *TFAP2B* locus.

Analysis of the copy number status of *TFAP2B* in 199 primary neuroblastoma samples using aCGH revealed that the *TFAP2B* locus is mostly not affected by genomic copy number alterations, and that *TFAP2B* copy numbers and *TFAP2B* expression are not correlated (Supplementary Figure S5). We also did not detect any somatic mutations affecting *TFAP2B* in primary neuroblastoma using whole-genome (n = 30) and whole-exome (n = 125) massive parallel sequencing data (unpublished data). Together, our data indicate that neither copy number alterations nor somatic mutations of *TFAP2B* are a major cause of reduced *TFAP2B* expression levels in unfavorable neuroblastoma.

3.3. TFAP2B expression is associated with RA responsiveness in neuroblastoma cell lines

To examine the role of *TFAP2B* in neuroblastoma pathogenesis, we first screened thirteen neuroblastoma cell lines for endogenous TFAP2B expression both on the RNA and protein level, and categorized them as *TFAP2B*^{high} (SK-N-BE(2)c, SH-SY5Y, LAN-5, CLB-GA, NBL-S and Kelly), *TFAP2B*^{intermediate} (IMR-32, NMB and SK-N-DZ) and *TFAP2B*^{low} (CHP-212, SH-EP, GI-ME-N and SK-N-AS; Figure 3a and Supplementary Figure S6). Next, we asked whether *TFAP2B* expression of cell

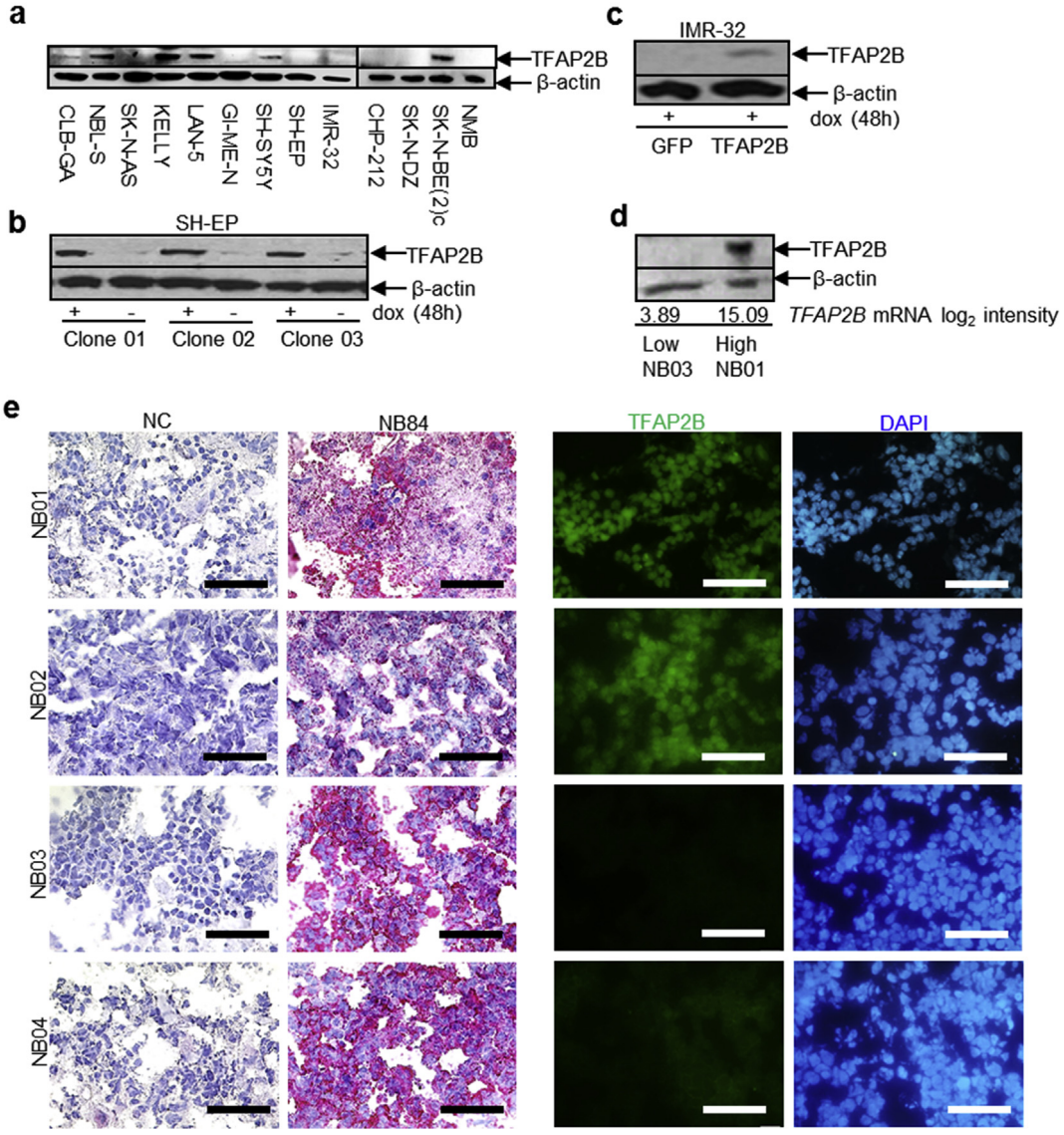

Figure 3 – TFAP2B protein level in neuroblastoma cell lines and primary tumors. (a) Endogenous TFAP2B protein level in neuroblastoma cell lines. (b) Inducible expression of TFAP2B in SH-EP cell clones. (c) Inducible expression of TFAP2B and GFP in IMR-32 cells. (d) TFAP2B protein level in primary neuroblastoma samples; NB01 with high and NB03 with low *TFAP2B* mRNA expression according to microarray analysis. (e) Immunohistochemical staining of the neuroblastoma-specific marker NB84 in four primary neuroblastoma samples (left panel; scale bar = 50 μm), and immunofluorescence staining of TFAP2B in the consecutive sections of the same samples (right panel; scale bar = 50 μm). NC, negative control.

lines correlates with their responsiveness to RA. For this purpose, we evaluated morphological signs of differentiation and expression levels of the neuronal marker genes microtubule associated protein 2 (*MAP2*) and neurofilament middle chain (*NEFM*) in response to RA treatment. We found that neuronal marker genes were up-regulated upon RA treatment in all six *TFAP2B*^{high} cell lines, which was accompanied by induction of neurite-like processes in five of them (Supplementary Figure S7). Likewise, signs of differentiation were readily detectable in the *TFAP2B*^{intermediate} cell lines IMR-32 and NMB (Supplementary Figure S8), while SK-N-DZ cells died rapidly upon RA treatment (not shown). By contrast, we did not detect any signs of neuronal differentiation upon RA treatment in *TFAP2B*^{low} cell lines (Supplementary Figure S9). Contrary to *TFAP2B*, expression levels of the RA responsive genes *RARB* and *CRABP2* were neither associated with RA sensitivity of the cell lines nor with *TFAP2B* expression (Supplementary Figure S10).

We also evaluated the expression dynamics of *TFAP2B* after RA treatment in *TFAP2B*^{high} SK-N-BE(2)c cells and *TFAP2B*^{intermediate} NMB and IMR-32 cells. In all three cell lines, *TFAP2B* levels decreased upon RA treatment (Supplementary Figure S11). This finding is in line with *TFAP2B* expression patterns in primary neuroblastoma, which was highest in poorly differentiated tumors (Supplementary Figure S3a), indicating that high TFAP2B expression may be associated with a specific developmental stage of the progenitor cells, as suggested previously (Bourdeaut et al., 2009). Together with the fact that endogenous *TFAP2B* expression is closely associated with RA responsiveness of neuroblastoma cell lines, our data suggest that TFAP2B expression might represent rather a precondition to induce RA-mediated differentiation programs than a downstream target of RA in neuroblastoma.

3.4. *TFAP2B re-expression impairs proliferation and cell cycle progression in neuroblastoma cell lines*

To further evaluate the role of TFAP2B in neuroblastoma pathogenesis, *TFAP2B* expression was reconstituted in two cell lines (IMR-32 and SH-EP) using an inducible retroviral gene transfer system. Doxycycline-induced TFAP2B protein levels in the cell lines were comparable to physiological protein levels observed in primary neuroblastomas with high *TFAP2B* expression (Figure 3b–e).

In SH-EP cells, the effect of TFAP2B on neuroblastoma cell growth was explored in three stable clones allowing doxycycline-inducible TFAP2B expression, whereas polyclonal TFAP2B expressing IMR-32 cells were compared with polyclonal GFP-expressing controls. We observed a significant reduction in proliferation after TFAP2B induction in both cell lines (Figure 4 and Supplementary Figure S12a). To determine whether reduced proliferation upon TFAP2B re-expression might be due to impaired cell cycle progression, the DNA content of TFAP2B-expressing cells was assessed by flow cytometry. We found a significant increase of the G0/G1 peak at day 6 after TFAP2B induction in both IMR-32 cells and SH-EP cells (Figure 4 and Supplementary Figure S12b), indicating that TFAP2B re-expression impairs cell cycle progression from G1 to S phase. We also detected a significant increase of the sub-G1 fraction after TFAP2B induction in IMR-32 cells

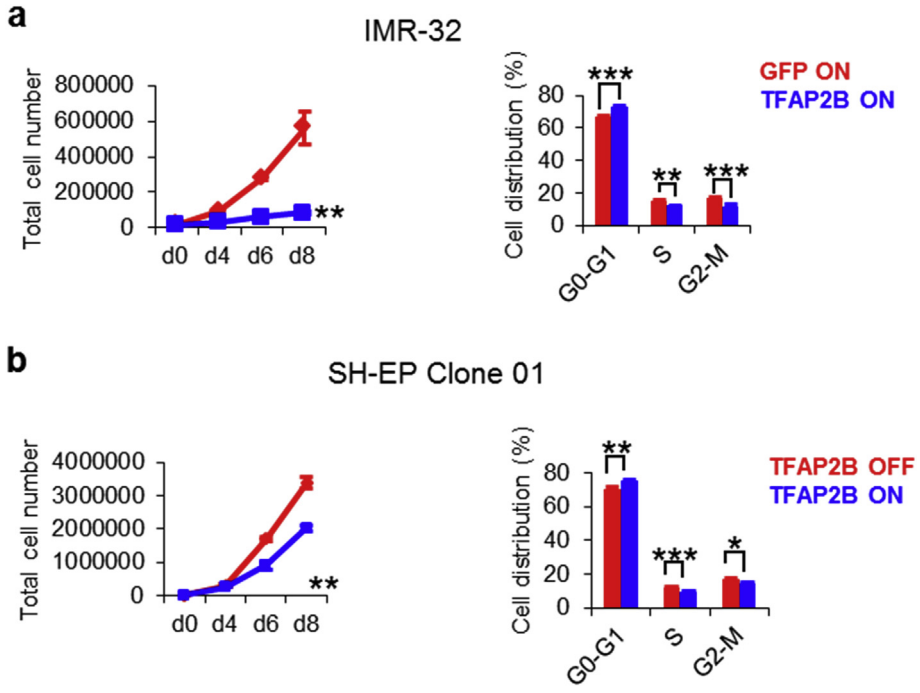

Figure 4 – *TFAP2B* re-expression inhibits growth of neuroblastoma cells. (a) Proliferation of IMR-32 and SH-EP cells upon TFAP2B re-expression as assessed by trypan blue dye exclusion analysis. (b) Cell cycle analysis of IMR-32 and SH-EP cells at day 6 after TFAP2B induction as determined by FACS analysis. Fraction of cells in G0/G1 phase: SH-EP OFF, 69.05% ± 0.47%; SH-EP ON, 74.03% ± 0.26%, $p < 0.01$; IMR-32 *GFP*, 65.50% ± 0.84%; IMR-32 *TFAP2B*, 70.58% ± 0.59%, $p < 0.001$. Error bars indicate S.D; (n.s.), $p > 0.05$; (*), $p < 0.05$; (**), $p < 0.01$; (***), $p < 0.001$).

(Supplementary Figure S13a), indicating that cell death contributes to impaired proliferation in this cell line; a similar effect, however, was not observed in TFAP2B expressing SH-EP cells (Supplementary Figure S13b).

3.5. *TFAP2B induces neuronal differentiation in IMR-32 cells*

Microscopic inspection of TFAP2B-expressing IMR-32 cells revealed a high degree of morphological differentiation, as indicated by the development of neurite-like processes (Figure 5a). To further investigate whether this neuron-like morphology is associated with induction of neuronal markers, we measured expression levels of class III beta-tubulin (TUBB3) by immunofluorescence, and *MAP2*, *NEFM*, neuron specific enolase (*NSE*) and synaptophysin (*SYP*) by RT-qPCR, all of which were up-regulated in TFAP2B-expressing cells as compared to controls (Figure 5b,c). Similarly, expression levels of *DBH* and *TH* were induced upon TFAP2B re-expression (Figure 5d), suggesting that cells differentiate into a noradrenergic phenotype.

By contrast, we did not observe morphological differentiation in TFAP2B expressing SH-EP cells (Supplementary Figure S14a). Consistent with this finding, up-regulation of the markers TUBB3, *MAP2* and *DBH* was lacking (Supplementary Figure S14b–d). We found, however, that impaired proliferation and G1-arrest was associated with cellular senescence after TFAP2B induction in SH-EP cells as

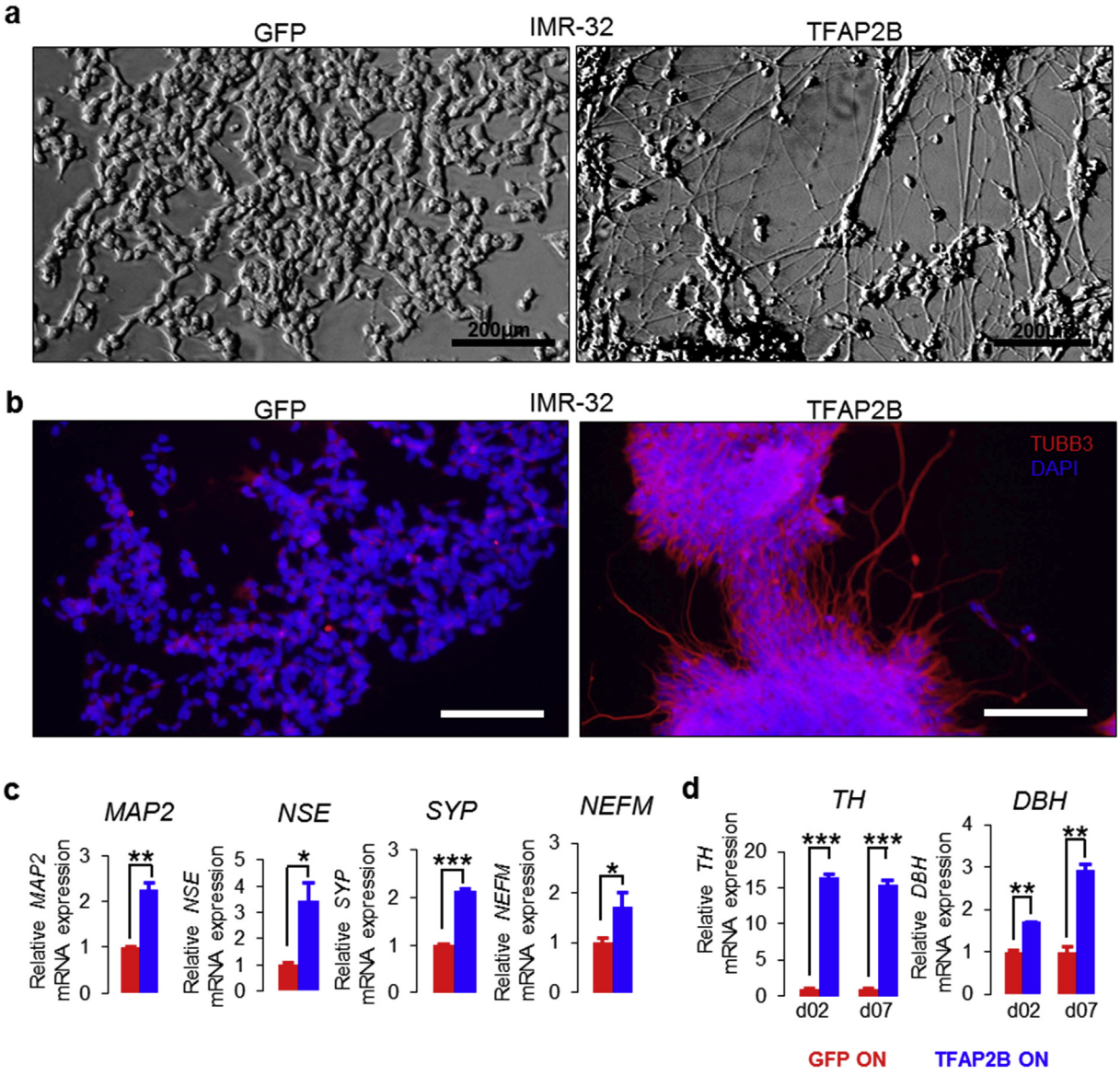

Figure 5 – TFAP2B induces neuronal differentiation in IMR-32 cells. (a) Morphological changes of IMR-32 cells upon TFAP2B and GFP induction. Bright filed; Scale bar = 200 µm. (b) Immunofluorescence staining of TUBB3 in IMR-32 after TFAP2B and GFP induction. Scale bar = 75 µm; Red = TUBB3; Blue = DAPI. (c) Analysis of the neuron-related markers *MAP2, NSE, SYP* and *NEFM* in IMR-32 cells upon *TFAP2B* re-expression by RT-qPCR. (d) Analysis of *TH* and *DBH* in IMR-32 cells after *TFAP2B* re-expression by RT-qPCR. Error bars indicate S.D; (n.s.), $p > 0.05$; (*), $p < 0.05$; (**), $p < 0.01$; (***), $p < 0.001$).

assessed by acidic β-galactosidase (SA-β-Gal) activity analysis (Supplementary Figure S15).

Given the fact that methylation of CpG sites in proximity to the *TFAP2B* transcription start site was strongly correlated with low *TFAP2B* expression levels in primary neuroblastomas, we wondered whether treatment of IMR-32 cells with the DNA methyltransferase inhibitor 5-aza-2′-deoxycytidine (DAC) may result in a similar phenotype as observed after transgenic *TFAP2B* re-expression. After 3 days of DAC treatment, we indeed detected significantly increased *TFAP2B* expression levels, as well as induction of *MAP2* and *NEFM* as compared to the controls (Supplementary Figure S16a and S16b). We also observed induction of neurite-like processes and significant reduction in proliferation upon DAC treatment, which was followed, however, by death of the majority of cells (Supplementary Figure S16c and S16d). Accordingly, we found a significant increase of the sub-G1 fraction along with a G2/M arrest of DAC treated cells (Supplementary Figure S16e), analogous to previous observations in other cancer entities (Shin et al., 2013). Together, these findings further substantiate that *TFAP2B* may be silenced by promoter methylation in unfavorable neuroblastoma.

3.6. *Microarray-based gene expression analysis of IMR-32 cells upon TFAP2B induction*

To gain insight into TFAP2B related mechanisms driving growth arrest and differentiation in IMR-32 cells, we performed microarray-based gene expression analysis at days 2 and 7 after *TFAP2B* induction in comparison to GFP vector control cells. Gene set enrichment analysis revealed that, among the entire curated pathway gene set collection, the Biocarta cell cycle pathway gene set was the most significant gene set enriched in TFAP2B samples (normalized enrichment score, 1.59; p = 0.016; Supplementary Figure S17a). Among the genes in this set, we observed that expression of the cell cycle inhibitor gene *CDKN2A* was significantly induced in TFAP2B expressing cells. By contrast, expression of the cyclin-dependent kinase genes *CDK4* and *CDK6* decreased upon TFAP2B re-expression, supporting the notion of impaired cell cycle progression in TFAP2B expressing cells.

Furthermore, microarray-based expression analysis validated up-regulation of the neuronal marker genes investigated in this study (*TUBB3*, *MAP2*, *NEFM*, *NSE*, *SYP*, *DBH* and *TH*) and the catecholamine biosynthesizing enzyme genes *DBH* and *TH* (Supplementary Figure S17b). In addition, we found TFAP2B mediated induction of the neurotrophin receptor gene *NTRK1*, which has been implicated in neuroblastoma differentiation and regression and is strongly associated with favorable patient outcome (Brodeur, 2003). By contrast, the RE1-silencing transcription factor *REST*, a master repressor of neuronal genes (Thiel et al., 2015), was persistently down-regulated upon TFAP2B induction, indicating that TFAP2B enables differentiation in neuroblastoma cells by repression of REST.

Since TFAP2 transcription factors have been described to act as a negative regulator of Myc-mediated transactivation (Gaubatz et al., 1995), we also assessed *TFAP2B* and *MYCN* expression in primary neuroblastoma and in cell line models. In primary tumors, *TFAP2B* and *MYCN* expression levels were inversely correlated (Figure 1c and Supplementary Figure S18a). In line with this observation, *MYCN* was down-regulated in IMR-32 cells upon *TFAP2B* expression (Supplementary Figure S17b), while *TFAP2B* was down-regulated upon *MYCN* induction in SH-SY5Y, a non-*MYCN* amplified cell line with high endogenous TFAP2B expression

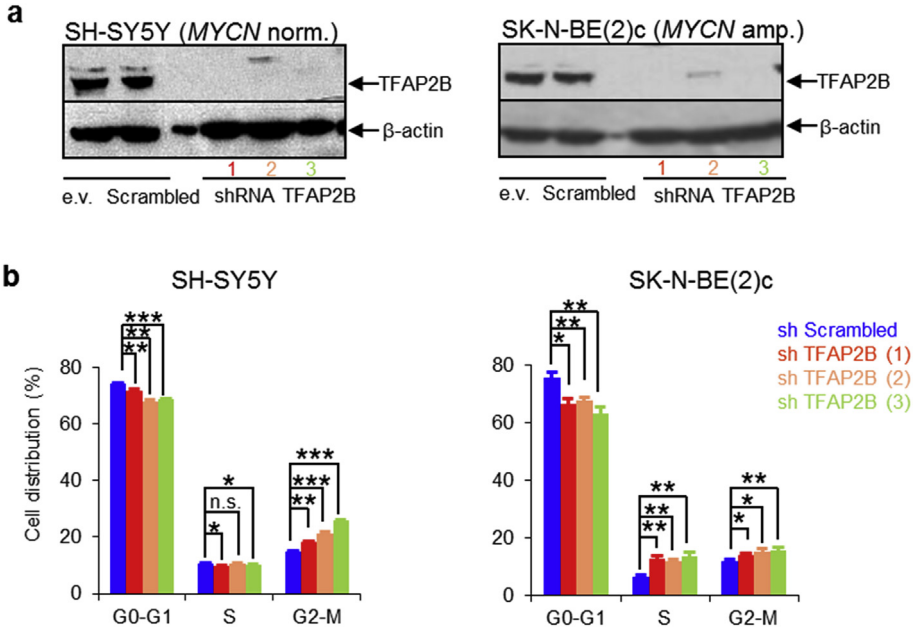

Figure 6 – Knockdown of TFAP2B accelerates cell cycle progression upon RA treatment in neuroblastoma cells. (a) Knockdown efficiency of TFAP2B in SH-SY5Y and SK-N-BE(2)c cells as determined by Western blot analysis; e.v., empty vector control. (b) Cell cycle analysis of SH-SY5Y and SK-N-BE(2)c cells after treatment with 1 μM RA for 6 days and 10 days, respectively. Error bars indicate S.D; (*), $p < 0.05$; (**), $p < 0.01$; (***), $p < 0.001$.

(Supplementary Figure S18b and S18c). Together, these data suggest that *TFAP2B* and *MYCN* affect each other reciprocally by direct or indirect repression, thereby promoting a favorable and an unfavorable tumor phenotype, respectively.

3.7. *Knockdown of TFAP2B abrogates RA-induced neuronal differentiation*

To validate the significance of TFAP2B in neuronal differentiation of neuroblastoma, we evaluated whether silencing of *TFAP2B* using lentiviral shRNAs in SK-N-BE(2)c and SH-SY5Y neuroblastoma cells may impair RA induced neuronal differentiation. These two cell lines express high endogenous TFAP2B protein levels (Figure 3a) and are known to differentiate in response to RA into neuronal type cells (Supplementary Figure S7) (Jeong et al., 2006; Rebhan et al., 1994). We tested 4 lentiviral constructs expressing short hairpin RNA sequences against human *TFAP2B* (sh*TFAP2B*), and three of them significantly reduced TFAP2B protein levels in both SH-SY5Y and SK-N-BE(2)c cells (Figure 6a). The effects of RA treatment were assessed in both cell lines after TFAP2B knockdown and in control cells. Upon TFAP2B knockdown, we observed a significant reduction of cells in the G1 phase of the cell cycle in both RA-treated SH-SY5Y and SK-N-BE(2)c cells (Figure 6b and Supplementary Figure S19). Furthermore, morphological signs of neuronal differentiation were readily detectable in RA-treated control cells, but absent in neuroblastoma cells lacking TFAP2B expression (Figure 7, Supplementary Figures S20 and S21). In addition, knockdown of TFAP2B severely impaired up-regulation of the neuronal markers MAP2 (Figure 8a, Supplementary Figures S22 and S23) as well as *NEFM* and *SYP* (Figure 8b and 8c). In line with these findings, we found that expression of *DBH* was significantly diminished in both RA-treated SH-SY5Y and SK-N-BE(2)c cells after TFAP2B knock-down in comparison to the controls (Figure 8b and 8c). Similarly, expression of *TH* was down-regulated in RA-treated SK-N-BE(2)c cells after TFAP2B knock-down, while *TH* expression levels was not measurable by RT-qPCR in SH-SY5Y cells in our study. Together, the reverse phenotypes observed in RA-treated neuroblastoma cells after TFAP2B knockdown and in recombinant TFAP2B expressing neuroblastoma cells suggest that TFAP2B is playing a vital role in retaining RA responsiveness and in mediating differentiation into a noradrenergic neuronal phenotype in neuroblastoma.

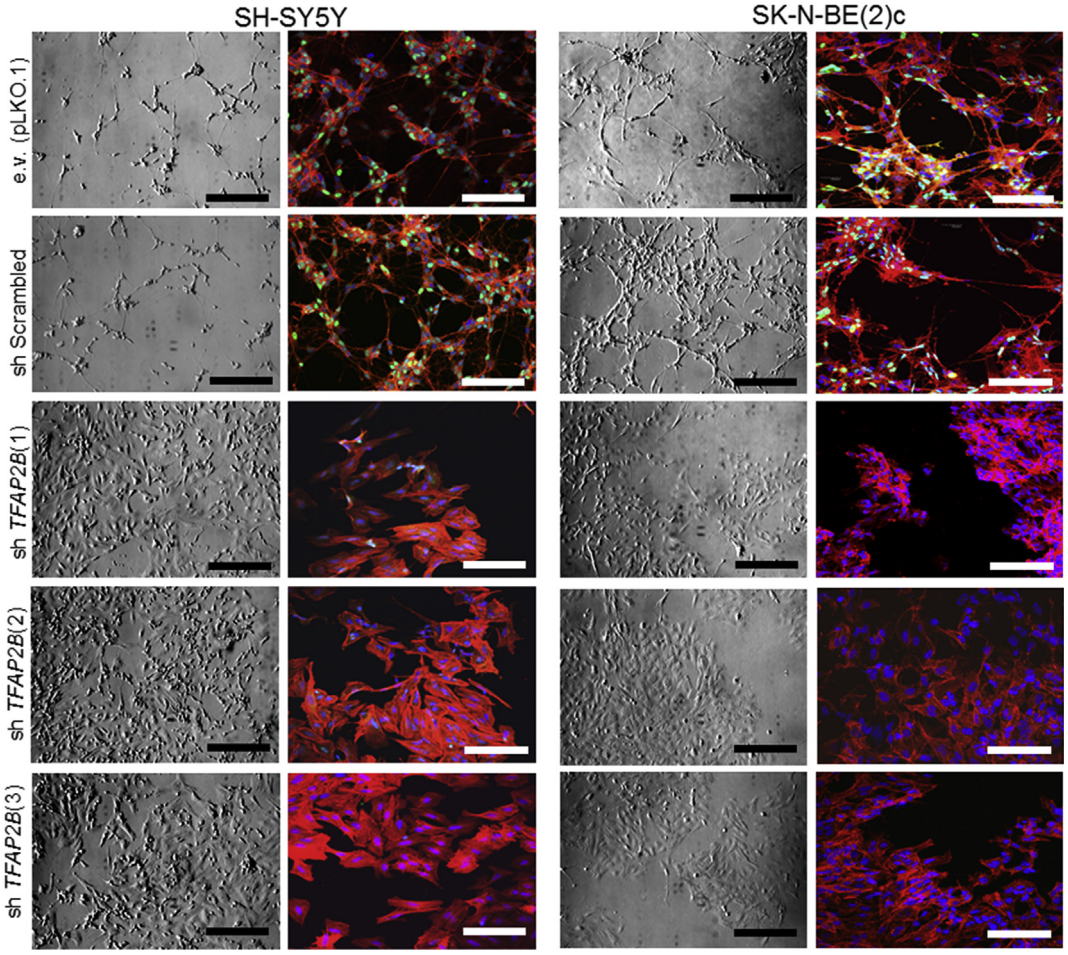

Figure 7 – Knockdown of TFAP2B abrogates RA-induced neuronal differentiation in neuroblastoma cells. Morphological changes in SH-SY5Y and SK-N-BE(2)c cells after treatment with 1 μM RA for 6 and 10 days, respectively. Left panel, bright field; scale bar = 200 μm; right panel, fluorescent; scale bar = 50 μm; Green = TFAP2B; Red = actin filaments; Blue = DAPI.

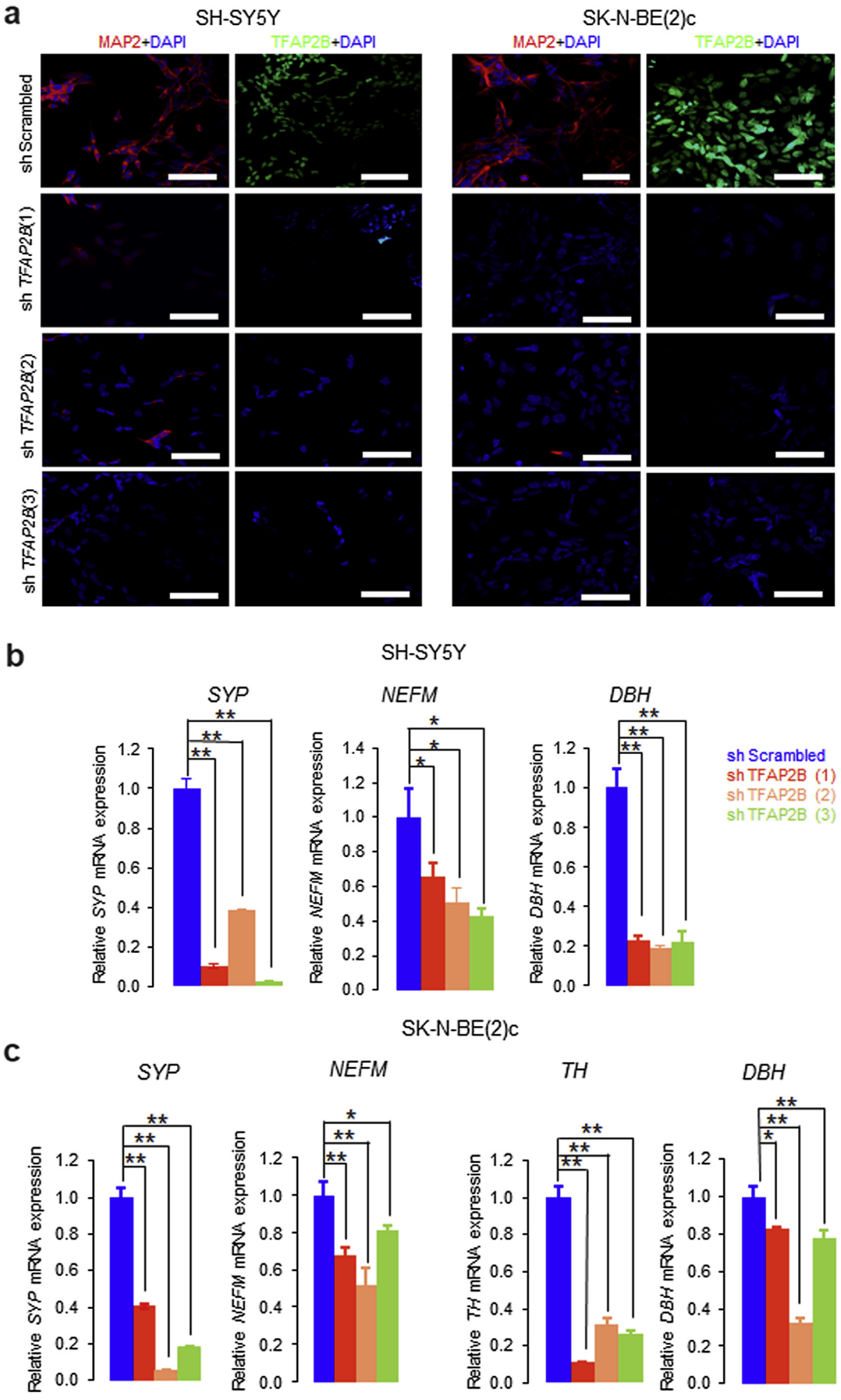

Figure 8 – Knockdown of TFAP2B leads to lack of upregulation of RA-induced neuronal differentiation markers in neuroblastoma cells. (a) Immunofluorescence staining of MAP2 in SH-SY5Y and SK-N-BE(2)c cells expressing shScrambled or shTFAP2B after RA treatment. Scale bar = 50 μm. (b) Analysis of neuronal differentiation markers *SYP*, *NEFM* and *DBH* in SH-SY5Y and (c) *SYP*, *NEFM*, *TH* and *DBH* in SK-N-BE(2)c cells expressing shScrambled or shTFAP2B after RA treatment by RT-qPCR. Error bars indicate S.D; (*), $p < 0.05$; (**), $p < 0.01$.

4. Discussion

Neuroblastoma is a pediatric solid tumor that originates from embryonal neural crest cells committed to the development of the sympathetic nervous system. In most cases, neuroblastoma presents as a tumor consisting of poorly differentiated small round blue cells, which may, however, differentiate into more benign tumor phenotypes (i.e., ganglioneuroblastoma or ganglioneuroma) either spontaneously or following cytotoxic treatment. Since many transcriptional regulators (e.g., PHOX2B, MYCN) involved in developmental differentiation processes are dysregulated in this malignancy (Nakagawara and Ohira, 2004), it has been suggested that the physiologic program of neuroblast differentiation and growth control is disrupted in neuroblastoma (Nakagawara et al., 1993). We here provide further evidence for this hypothesis by showing that the developmental transcription factor TFAP2B is significantly involved in mediating neuroblastoma differentiation.

In our study, we demonstrate that high *TFAP2B* expression levels are strongly associated with favorable prognostic characteristics and beneficial outcome in neuroblastoma. In neuroblastoma cell line models, re-expression of TFAP2B led to impaired cell cycle progression associated with noradrenergic neuronal differentiation or senescence. TFAP2B re-expression in IMR-32 cells was accompanied by down-regulation of *MYCN* and *REST*, suggesting that direct or indirect repression of transcription factors critically involved in sympathoadrenal development may promote TFAP2B mediated differentiation in neuroblastoma (Marshall et al., 2014). Our observations are in line with previous reports, in which *TFAP2B* was found to be predominantly expressed in the sympathetic ganglia of developing mouse embryos, pointing towards its role in sympathetic nervous system development (Hong et al., 2008). In addition, knock-out of *Tfap2b* in transgenic mice significantly impaired the development of sympathetic ganglia, while forced *TFAP2B* expression in chick neural crest stem cells favored their differentiation into sympathoadrenergic cells (Hong et al., 2008). In another murine knock-out model, *Tfap2b* was found to be essential for the survival of migrating neural crest cells committed to the development of sympathetic neurons (Schmidt et al., 2011). Together, our data suggest that TFAP2B contributes to a favorable phenotype and noradrenergic neuronal differentiation in neuroblastoma, which may reflect its physiological role during sympathetic nervous system development.

We also observed that knockdown of *TFAP2B* abrogates neuronal differentiation of the tumor cells in the presence of RA. The signaling molecule RA has been shown to induce differentiation of neuroblastoma cells in experimental systems, which has led to the integration of RA-based maintenance therapies in current treatment protocols to prevent relapse (Matthay et al., 1999). The mechanisms underlying spontaneous and RA-induced neuroblastoma differentiation are, however, still poorly understood. We here provide evidence that TFAP2B expression may be necessary to enable RA-mediated differentiation of neuroblastoma cells, indicating that TFAP2B and RA may cooperate in promoting neuronal differentiation in neuroblastoma. Induction of *TFAP2* expression upon RA treatment has been previously shown to occur during neuroectodermal differentiation of embryonal carcinoma cells, while it was absent during mesoendodermal differentiation (Philipp et al., 1994). In contrast to these observations, we found that *TFAP2B* expression was down-regulated in RA treated neuroblastoma cells, suggesting that *TFAP2B* expression is rather a precondition to enable RA-mediated differentiation than a downstream target of RA in neuroblastoma. In line with the latter hypothesis, we found highest *TFAP2B* levels in poorly differentiated tumors, while it was lower in differentiating and stroma-rich tumors, as reported previously (Albino et al., 2008; Bourdeaut et al., 2009). Thus, our data are in support of the notion that TFAP2B expression is associated with a specific developmental stage of the neuroblastoma progenitor cells (Bourdeaut et al., 2009), which may render the tumor cells susceptible to signaling molecules inducing neuronal differentiation.

We did not find any evidence of genetic alterations of the *TFAP2B* locus, but noticed that methylation of CpG sites in the 5′ region of *TFAP2B* is associated with low *TFAP2B* expression and unfavorable prognostic markers. We also observed up-regulation of *TFAP2B* and neuronal markers in IMR-32 neuroblastoma cells upon treatment with the DNA methyltransferase inhibitor DAC. These data may suggest that *TFAP2B* is silenced by DNA methylation of CpG sites at the *TFAP2B* locus. In neuroblastoma, gene repression by genomic methylation has been shown to be involved in several putative tumor suppressor genes (Abe et al., 2005; Decock et al., 2012; Michalowski et al., 2008). In addition, aberrant DNA methylation of TFAP2 family members and induction of their expression upon DAC treatment have been described previously in cancer (Douglas et al., 2004; Tong et al., 2010). Another recent study reported that CpG sites at the *TFAP2B* locus are highly methylated in esophageal squamous cell carcinoma but not in normal esophageal mucosa (Takahashi et al., 2013). Together, these data point towards genomic DNA methylation as a mechanism to silence *TFAP2B* expression in neuroblastoma. Alternatively, other molecular mechanisms, such as upstream transcriptional regulators or microRNAs, may also contribute to regulating expression levels of *TFAP2B* (Plouhinec et al., 2014).

In conclusion, our results point towards a vital role of TFAP2B in mediating noradrenergic neuronal differentiation in neuroblastoma and in retaining RA responsiveness, and indicate that *TFAP2B* expression is silenced by aberrant DNA methylation in high risk neuroblastoma. Our data may be used as a starting point to further elucidate the molecular mechanisms of neuroblastoma differentiation, which may eventually lead to the development of biomarker-based patient stratification systems for differentiation treatment strategies.

Conflict of interest

The authors have no conflict of interest to declare.

Acknowledgements

The authors thank Andrea Krämer for valuable suggestions and Mirjam Koker for helping us with the lentiviral mediated

knockdown experiments. This work was supported by grants from the Cologne Center for Molecular Medicine Cologne (CMMC); the Bundesministerium für Bildung und Forschung (BMBF) through the National Genome Research Network plus (NGFNplus, Grant No. 01GS0895 to MF and Grant No. 01GS0896 to KOH and FW) and through the e:Med initiative (Grant No. 01ZX1303A to MF and Grant No. 01ZX1307D to MF and FW); the Fördergesellschaft Kinderkrebs-Neuroblastom-Forschung e.V.; the Competence Network Pediatric Oncology and Hematology (KPOH); the EU (FP6) E.E.T. Pipeline (Grant No. 037260 to DD and FW); the EU (FP7) Asset (Grant No. 259348 to DD and FW); the BMBF MYC-NET, CancerSys (Grant No. 0316076A to DD and FW). We are thankful to HEC Pakistan and DAAD for 4 years PhD scholarship to FI.

Appendix A. Supplementary data

Supplementary data related to this article can be found at http://dx.doi.org/10.1016/j.molonc.2015.10.020.

REFERENCES

Abe, M., Ohira, M., Kaneda, A., Yagi, Y., Yamamoto, S., Kitano, Y., Takato, T., Nakagawara, A., Ushijima, T., 2005. CpG island methylator phenotype is a strong determinant of poor prognosis in neuroblastomas. Cancer Res. 65, 828–834.

Albino, D., Scaruffi, P., Moretti, S., Coco, S., Truini, M., Di Cristofano, C., Cavazzana, A., Stigliani, S., Bonassi, S., Tonini, G.P., 2008. Identification of low intratumoral gene expression heterogeneity in neuroblastic tumors by genome-wide expression analysis and game theory. Cancer 113, 1412–1422.

Auman, H.J., Nottoli, T., Lakiza, O., Winger, Q., Donaldson, S., Williams, T., 2002. Transcription factor AP-2gamma is essential in the extra-embryonic lineages for early postimplantation development. Development 129, 2733–2747.

Bourdeaut, F., Janoueix-Lerosey, I., Lucchesi, C., Paris, R., Ribeiro, A., de Pontual, L., Amiel, J., Lyonnet, S., Pierron, G., Michon, J., Peuchmaur, M., Delattre, O., 2009. Cholinergic switch associated with morphological differentiation in neuroblastoma. J. Pathol. 219, 463–472.

Brodeur, G.M., 2003. Neuroblastoma: biological insights into a clinical enigma. Nature reviews. Cancer 3, 203–216.

Brodeur, G.M., Pritchard, J., Berthold, F., Carlsen, N.L., Castel, V., Castelberry, R.P., De Bernardi, B., Evans, A.E., Favrot, M., Hedborg, F., et al., 1993. Revisions of the international criteria for neuroblastoma diagnosis, staging, and response to treatment. J. Clin. Oncol. 11, 1466–1477.

Cohn, S.L., Pearson, A.D., London, W.B., Monclair, T., Ambros, P.F., Brodeur, G.M., Faldum, A., Hero, B., Iehara, T., Machin, D., Mosseri, V., Simon, T., Garaventa, A., Castel, V., Matthay, K.K., 2009. The international neuroblastoma risk group (INRG) classification system: an INRG Task Force report. J. Clin. Oncol. 27, 289–297.

De Preter, K., Vandesompele, J., Heimann, P., Yigit, N., Beckman, S., Schramm, A., Eggert, A., Stallings, R.L., Benoit, Y., Renard, M., De Paepe, A., Laureys, G., Pahlman, S., Speleman, F., 2006. Human fetal neuroblast and neuroblastoma transcriptome analysis confirms neuroblast origin and highlights neuroblastoma candidate genes. Genome Biol. 7, R84.

Decock, A., Ongenaert, M., Hoebeeck, J., De Preter, K., Van Peer, G., Van Criekinge, W., Ladenstein, R., Schulte, J.H., Noguera, R., Stallings, R.L., Van Damme, A., Laureys, G., Vermeulen, J., Van Maerken, T., Speleman, F., Vandesompele, J., 2012. Genome-wide promoter methylation analysis in neuroblastoma identifies prognostic methylation biomarkers. Genome Biol. 13, R95.

Douglas, D.B., Akiyama, Y., Carraway, H., Belinsky, S.A., Esteller, M., Gabrielson, E., Weitzman, S., Williams, T., Herman, J.G., Baylin, S.B., 2004. Hypermethylation of a small CpGuanine-rich region correlates with loss of activator protein-2alpha expression during progression of breast cancer. Cancer Res. 64, 1611–1620.

Eckert, D., Buhl, S., Weber, S., Jager, R., Schorle, H., 2005. The AP-2 family of transcription factors. Genome Biol. 6, 246.

Fischer, M., Bauer, T., Oberthur, A., Hero, B., Theissen, J., Ehrich, M., Spitz, R., Eils, R., Westermann, F., Brors, B., Konig, R., Berthold, F., 2010. Integrated genomic profiling identifies two distinct molecular subtypes with divergent outcome in neuroblastoma with loss of chromosome 11q. Oncogene 29, 865–875.

Fischer, M., Oberthuer, A., Brors, B., Kahlert, Y., Skowron, M., Voth, H., Warnat, P., Ernestus, K., Hero, B., Berthold, F., 2006. Differential expression of neuronal genes defines subtypes of disseminated neuroblastoma with favorable and unfavorable outcome. Clin. Cancer Res. 12, 5118–5128.

Fischer, M., Skowron, M., Berthold, F., 2005. Reliable transcript quantification by real-time reverse transcriptase-polymerase chain reaction in primary neuroblastoma using normalization to averaged expression levels of the control genes HPRT1 and SDHA. J. Mol. Diagn. 7, 89–96.

Fredlund, E., Ringner, M., Maris, J.M., Pahlman, S., 2008. High Myc pathway activity and low stage of neuronal differentiation associate with poor outcome in neuroblastoma. Proc. Natl. Acad. Sci. U. S. A. 105, 14094–14099.

Fu, L., Shi, K., Wang, J., Chen, W., Shi, D., Tian, Y., Guo, W., Yu, W., Xiao, X., Kang, T., Wang, S., Huang, W., Deng, W., 2014. TFAP2B overexpression contributes to tumor growth and a poor prognosis of human lung adenocarcinoma through modulation of ERK and VEGF/PEDF signaling. Mol. Cancer 13, 89.

Gaubatz, S., Imhof, A., Dosch, R., Werner, O., Mitchell, P., Buettner, R., Eilers, M., 1995. Transcriptional activation by Myc is under negative control by the transcription factor AP-2. EMBO J. 14, 1508–1519.

Hong, S.J., Huh, Y.H., Leung, A., Choi, H.J., Ding, Y., Kang, U.J., Yoo, S.H., Buettner, R., Kim, K.S., 2011. Transcription factor AP-2beta regulates the neurotransmitter phenotype and maturation of chromaffin cells. Mol. Cell Neurosciences 46, 245–251.

Hong, S.J., Lardaro, T., Oh, M.S., Huh, Y., Ding, Y., Kang, U.J., Kirfel, J., Buettner, R., Kim, K.S., 2008. Regulation of the noradrenaline neurotransmitter phenotype by the transcription factor AP-2beta. J. Biol. Chem. 283, 16860–16867.

Hothorn, T., Lausen, B., 2002. On the exact distribution of maximally selected rank statistics. Comput. Stat. Data Anal. 43, 121–137.

Jeong, H., Kim, M.S., Kim, S.W., Kim, K.S., Seol, W., 2006. Regulation of tyrosine hydroxylase gene expression by retinoic acid receptor. J. Neurochem. 98, 386–394.

Kocak, H., Ackermann, S., Hero, B., Kahlert, Y., Oberthuer, A., Juraeva, D., Roels, F., Theissen, J., Westermann, F., Deubzer, H., Ehemann, V., Brors, B., Odenthal, M., Berthold, F., Fischer, M., 2013. Hox-C9 activates the intrinsic pathway of apoptosis and is associated with spontaneous regression in neuroblastoma. Cell Death Dis. 4, e586.

Lausen, B., Schumacher, M., 1992. Maximally selected rank statistics. Biometrics 48, 73–85.

Luscher, B., Mitchell, P.J., Williams, T., Tjian, R., 1989. Regulation of transcription factor AP-2 by the morphogen retinoic acid and by second messengers. Genes Development 3, 1507–1517.

Marshall, G.M., Carter, D.R., Cheung, B.B., Liu, T., Mateos, M.K., Meyerowitz, J.G., Weiss, W.A., 2014. The prenatal origins of cancer. Nature reviews. Cancer 14, 277–289.

Matthay, K.K., Reynolds, C.P., Seeger, R.C., Shimada, H., Adkins, E.S., Haas-Kogan, D., Gerbing, R.B., London, W.B., Villablanca, J.G., 2009. Long-term results for children with high-risk neuroblastoma treated on a randomized trial of myeloablative therapy followed by 13-cis-retinoic acid: a children's oncology group study. J. Clin. Oncol. 27, 1007–1013.

Matthay, K.K., Villablanca, J.G., Seeger, R.C., Stram, D.O., Harris, R.E., Ramsay, N.K., Swift, P., Shimada, H., Black, C.T., Brodeur, G.M., Gerbing, R.B., Reynolds, C.P., 1999. Treatment of high-risk neuroblastoma with intensive chemotherapy, radiotherapy, autologous bone marrow transplantation, and 13-cis-retinoic acid. Children's Cancer Group. N. Engl. J. Med. 341, 1165–1173.

Michalowski, M.B., de Fraipont, F., Plantaz, D., Michelland, S., Combaret, V., Favrot, M.C., 2008. Methylation of tumor-suppressor genes in neuroblastoma: the RASSF1A gene is almost always methylated in primary tumors. Pediatr. Blood Cancer 50, 29–32.

Miettinen, M., Chatten, J., Paetau, A., Stevenson, A., 1998. Monoclonal antibody NB84 in the differential diagnosis of neuroblastoma and other small round cell tumors. Am. J. Surg. Pathol. 22, 327–332.

Moser, M., Pscherer, A., Roth, C., Becker, J., Mucher, G., Zerres, K., Dixkens, C., Weis, J., Guay-Woodford, L., Buettner, R., Fassler, R., 1997. Enhanced apoptotic cell death of renal epithelial cells in mice lacking transcription factor AP-2beta. Genes Development 11, 1938–1948.

Nakagawara, A., Arima-Nakagawara, M., Scavarda, N.J., Azar, C.G., Cantor, A.B., Brodeur, G.M., 1993. Association between high levels of expression of the TRK gene and favorable outcome in human neuroblastoma. N. Engl. J. Med. 328, 847–854.

Nakagawara, A., Ohira, M., 2004. Comprehensive genomics linking between neural development and cancer: neuroblastoma as a model. Cancer Lett. 204, 213–224.

Nowacki, S., Skowron, M., Oberthuer, A., Fagin, A., Voth, H., Brors, B., Westermann, F., Eggert, A., Hero, B., Berthold, F., Fischer, M., 2008. Expression of the tumour suppressor gene CADM1 is associated with favourable outcome and inhibits cell survival in neuroblastoma. Oncogene 27, 3329–3338.

Oberthuer, A., Juraeva, D., Hero, B., Volland, R., Sterz, C., Schmidt, R., Faldum, A., Kahlert, Y., Engesser, A., Asgharzadeh, S., Seeger, R., Ohira, M., Nakagawara, A., Scaruffi, P., Tonini, G.P., Janoueix-Lerosey, I., Delattre, O., Schleiermacher, G., Vandesompele, J., Speleman, F., Noguera, R., Piqueras, M., Benard, J., Valent, A., Avigad, S., Yaniv, I., Grundy, R.G., Ortmann, M., Shao, C., Schwab, M., Eils, R., Simon, T., Theissen, J., Berthold, F., Westermann, F., Brors, B., Fischer, M., 2015. Revised risk estimation and treatment stratification of low- and intermediate-risk neuroblastoma patients by integrating clinical and molecular prognostic markers. Clin. Cancer Res. 21, 1904–1915.

Oberthuer, A., Juraeva, D., Li, L., Kahlert, Y., Westermann, F., Eils, R., Berthold, F., Shi, L., Wolfinger, R.D., Fischer, M., Brors, B., 2010. Comparison of performance of one-color and two-color gene-expression analyses in predicting clinical endpoints of neuroblastoma patients. Pharmacogenomics J. 10, 258–266.

Ohira, M., Oba, S., Nakamura, Y., Isogai, E., Kaneko, S., Nakagawa, A., Hirata, T., Kubo, H., Goto, T., Yamada, S., Yoshida, Y., Fuchioka, M., Ishii, S., Nakagawara, A., 2005. Expression profiling using a tumor-specific cDNA microarray predicts the prognosis of intermediate risk neuroblastomas. Cancer Cell 7, 337–350.

Pellikainen, J.M., Kosma, V.M., 2007. Activator protein-2 in carcinogenesis with a special reference to breast cancer–a mini review. Int. J. Cancer 120, 2061–2067.

Philipp, J., Mitchell, P.J., Malipiero, U., Fontana, A., 1994. Cell type-specific regulation of expression of transcription factor AP-2 in neuroectodermal cells. Developmental Biol. 165, 602–614.

Plouhinec, J.L., Roche, D.D., Pegoraro, C., Figueiredo, A.L., Maczkowiak, F., Brunet, L.J., Milet, C., Vert, J.P., Pollet, N., Harland, R.M., Monsoro-Burq, A.H., 2014. Pax3 and Zic1 trigger the early neural crest gene regulatory network by the direct activation of multiple key neural crest specifiers. Developmental Biol. 386, 461–472.

Rebhan, M., Vacun, G., Bayreuther, K., Rosner, H., 1994. Altered ganglioside expression by SH-SY5Y cells upon retinoic acid-induced neuronal differentiation. Neuroreport 5, 941–944.

Reynolds, C.P., Matthay, K.K., Villablanca, J.G., Maurer, B.J., 2003. Retinoid therapy of high-risk neuroblastoma. Cancer Lett. 197, 185–192.

Schmidt, M., Huber, L., Majdazari, A., Schutz, G., Williams, T., Rohrer, H., 2011. The transcription factors AP-2beta and AP-2alpha are required for survival of sympathetic progenitors and differentiated sympathetic neurons. Developmental Biol. 355, 89–100.

Shimada, H., Ambros, I.M., Dehner, L.P., Hata, J., Joshi, V.V., Roald, B., 1999. Terminology and morphologic criteria of neuroblastic tumors: recommendations by the International Neuroblastoma Pathology Committee. Cancer 86, 349–363.

Shin, D.Y., Sung Kang, H., Kim, G.Y., Kim, W.J., Yoo, Y.H., Choi, Y.H., 2013. Decitabine, a DNA methyltransferases inhibitor, induces cell cycle arrest at G2/M phase through p53-independent pathway in human cancer cells. Biomed. Pharmacother. 67, 305–311.

Sidell, N., 1982. Retinoic acid-induced growth inhibition and morphologic differentiation of human neuroblastoma cells in vitro. J. Natl. Cancer Inst. 68, 589–596.

Spitz, R., Oberthuer, A., Zapatka, M., Brors, B., Hero, B., Ernestus, K., Oestreich, J., Fischer, M., Simon, T., Berthold, F., 2006. Oligonucleotide array-based comparative genomic hybridization (aCGH) of 90 neuroblastomas reveals aberration patterns closely associated with relapse pattern and outcome. Genes Chromosomes Cancer 45, 1130–1142.

Subramanian, A., Tamayo, P., Mootha, V.K., Mukherjee, S., Ebert, B.L., Gillette, M.A., Paulovich, A., Pomeroy, S.L., Golub, T.R., Lander, E.S., Mesirov, J.P., 2005. Gene set enrichment analysis: a knowledge-based approach for interpreting genome-wide expression profiles. Proc. Natl. Acad. Sci. U. S. A. 102, 15545–15550.

Takahashi, T., Matsuda, Y., Yamashita, S., Hattori, N., Kushima, R., Lee, Y.C., Igaki, H., Tachimori, Y., Nagino, M., Ushijima, T., 2013. Estimation of the fraction of cancer cells in a tumor DNA sample using DNA methylation. PloS One 8, e82302.

Thiel, G., Ekici, M., Rossler, O.G., 2015. RE-1 silencing transcription factor (REST): a regulator of neuronal development and neuronal/endocrine function. Cell Tissue Res. 359, 99–109.

Thomas, J.O., Nijjar, J., Turley, H., Micklem, K., Gatter, K.C., 1991. NB84: a new monoclonal antibody for the recognition of neuroblastoma in routinely processed material. J. Pathol. 163, 69–75.

Thorell, K., Bergman, A., Caren, H., Nilsson, S., Kogner, P., Martinsson, T., Abel, F., 2009. Verification of genes differentially expressed in neuroblastoma tumours: a study of potential tumour suppressor genes. BMC Med. Genomics 2, 53.

Tong, W.G., Wierda, W.G., Lin, E., Kuang, S.Q., Bekele, B.N., Estrov, Z., Wei, Y., Yang, H., Keating, M.J., Garcia-Manero, G., 2010. Genome-wide DNA methylation profiling of chronic lymphocytic leukemia allows identification of epigenetically

repressed molecular pathways with clinical impact. Epigenetics 5, 499–508.
Zeng, Y.X., Somasundaram, K., el-Deiry, W.S., 1997. AP2 inhibits cancer cell growth and activates p21WAF1/CIP1 expression. Nat. Genet. 15, 78–82.
Zhang, J., Hagopian-Donaldson, S., Serbedzija, G., Elsemore, J., Plehn-Dujowich, D., McMahon, A.P., Flavell, R.A., Williams, T., 1996. Neural tube, skeletal and body wall defects in mice lacking transcription factor AP-2. Nature 381, 238–241.